

*The Institute of Astronomy & Geophysics
of Mongolian Academy of Sciences*

Book of Extended Abstracts

The International Conference on Astronomy
and Geophysics in Mongolia, 2017

Ulaanbaatar, Mongolia
20-22 July, 2017

1957-2017
60 YEARS

**PROCEEDINGS OF THE INTERNATIONAL
CONFERENCE ON ASTRONOMY & GEOPHYSICS
IN MONGOLIA, 2017**

20-22 JULY, 2017, ULAANBAATAR, MONGOLIA

Extended Abstract Volume

Editors in chief

(Institute of Astronomy and Geophysics, Ulaanbaatar, Mongolia)

Prof. Demberel Sodnomsambuu

Dr. Odonbaatar Chimed

Dr. Ulziibat Munkhuu

Ulaanbaatar
2017

DDC
551.22
P-23

**INSTITUTE OF ASTRONOMY AND GEOPHYSICS OF MONGOLIAN
ACADEMY OF SCIENCES (IAG, MAS)**

Editors: Dr Odonbaatar Chimed
Dr Munkhsaikhan Adiya
Mrs Ankhtsetseg Dorjsuren

Print design: Mungunshagai Mendbayar

ISBN 978-99978-1-236-0

Published by Mongol Altay printing Co.ltd

ACTIVE FAULTS AND LATE CENOZOIC CRUSTAL STRESS STATE IN THE CENTRAL PART OF MONGOLIA

**Sankov V.A.^{1,2}, Parfeelevets A.V.¹, Miroshnichenko A.I.¹, Sankov A.V.¹,
Demberel S.³, Bayasgalan A.³ and Battogtokh D.³**

¹ Institute of the Earth Crust of Siberian Branch of Russian Academy of Sciences, Irkutsk, Russia

² Irkutsk State University, Irkutsk, Russia

³ Institute of Astronomy and Geophysics of Mongolian Academy of Sciences,
Lkhagvasuren street – 42, Maakhuur tolgoi, 5 khoro, BZD, 13343, Ulaanbaatar, Mongolia

Contact: sankov@crust.irk.ru

Abstract

The new data on the active faults of the Central Mongolia have been obtained that allow one to assess the deformation character of the continental crust in the transition zone from the region with predominance of the mountainous terrain (Western Mongolia) to the less elevated and active in the Cenozoic sub-platform area of Eastern Mongolia which is classified as the Amur lithospheric plate. The western boundary of the Amur plate is fragmentarily expressed in the tectonic structure. The beginning of the neotectonic activation of the faults varies from the Miocene in the Orkhon graben and the Pliocene in the Selenga depression to the Late Pleistocene in the Hangai-Hentei tectonic saddle. The traces of the Holocene fault activity were found in many sites. The active faults of the Hangai-Hentei tectonic saddle and the Burgut block form clusters. Among them the strike-slips and strike-slips with the revers component of the displacements dominate. The faults in the Selenga depression are concentrated in the extended zones such as the releasing band. The left-lateral strike-slips and normal faults prevail here. The reconstruction of the paleostress shows that the area between the Amur plate and the Mongolian block deforms under the compression and strike-slip conditions. The conditions of the extension and strike-slip are established in the Selenga depression and within the East Hangai dome.

Introduction

The territory of Mongolia is clearly divided into two parts. The western part is characterized by high velocities of the neotectonic movements and high seismic activity. The eastern part is characterized by relatively low velocities of the vertical neotectonic movements and weak scattered seismicity. According to [Zonenshain, Savostin, 1981], the latter refers to the part of the Amur lithospheric plate. The territory of our research is located in the Central Mongolia in the band between 101 and 105 meridians where many researchers draw the western boundary of the Amur plate (Fig. 1, insert). From south to north, 3 regions are distinguished in this band, differing in the features of the topography, the prevailing strike of the Late Cenozoic structures and the level of seismic activity. The Hangai-Hentei tectonic saddle (Fig. 1, rectangle 1) is characterized by a mid-mountain topography, a weak incision of river valleys which corresponds to a low level of the vertical tectonic movements and sporadic seismicity. The topography of the Burgut block (the Orkhon-Tola interfluvium) is more dissected (Fig. 1, rectangle 2). Seismic activity is high since in the western part of the block there was the epicenter of the Mogod earthquake in 1967 ($Mw = 7.0$) and its numerous aftershocks [One century of seismicity ..., 2000]. At the same time, the eastern part of the block is characterized by weak scattered seismicity. The topography of the uplifts around Selenga depression (Fig. 1, rectangle 3) is also dissected that indicates the relatively high velocity of the vertical movements. Within the massive block of the Buren-Nuruu uplift clusters of weak earthquakes and some earthquakes with a magnitude 5 are located. The structures of the Selenga depression are seismically weak at the present stage.

The Late Cenozoic fault tectonics and the tectonic stress field in the region have been poorly investigated. The tasks of our research include the identification of the active faults in the area, the assessment of their kinematics and the reconstruction of the paleostress state in the zones of these faults which will determine the style of the Late Cenozoic deformation of the earth's crust in the zone of the proposed interplate boundary.

Methods

Fault mapping and investigation of their kinematics was carried out using the interpretation of the space images and 3-D topography models (GTOPO-30). Field verification of the selected lineaments was carried out using the traditional geological-geomorphological and structural methods and was also accompanied by the study of the tectonic fracturing and microdisplacements in the zones of the active faults. For the paleostress state reconstruction the data on fractures and local faults with slicken slits and corrugations were collected. For the stress tensors of the tectonic paleostresses calculations we use the technology implemented in the WinTENSOR [Delvaux, 2012] software package.

Results

One of the important feature of the Late Cenozoic faulting of the area is the inheritance of the ancient linear heterogeneities by young structures. The faults of the Paleozoic and Mesozoic tectonic stages are inherited. In contrast the normal fault with the NE strike which controls the steep southeastern side of the Orkhon graben is laid regardless of the position of the main ancient inhomogeneities with NW strike [Geological map ..., 1998]. All major normal faults with NE strike widely distributed within the southern slope of the Hangai dome have the similar relationships with the main ancient structural inhomogeneities [Cunningham, 2001; Parfeevets, Sankov, 2012].

The Late Cenozoic activation of the faults in the area has signs of pronounced selectivity. Far from every zone of the mapped ancient fault, signs of deformations in the relief of the earth's surface are visible. The totality of the faults of the Hangai-Hentei tectonic saddle and the Burgut block can be classified as a cluster type of structures that represent a set of spatially proximate active faults having the similar kinematics patterns and locations in the field of the tectonic stresses. In the inner part of the Amur plate the cluster type of the active faults localization is replaced by sporadic that is represented by the randomly spatially distributed active faults.

The time of the onset of the neotectonic activation of the investigated faults is debatable. The formation of the Orkhon graben and the volcanism manifestation are observed from the end of the Miocene to the Middle Pleistocene [Rasskazov et al., 2012], it is associated with the activation of the expansion of the earth's crust. The movements along the Orkhon normal fault, as the main controlling structure, occurred from the Miocene up to the Holocene. In the Selenga depression the activation of the sublatitudinal and northeastern structures occurred in the Pliocene-Pleistocene [Khilko et al., 1985]. The fault deformations control the main forms of the topography. Several faults with the traces of Holocene activity were found. Within the Burgut block the latitudinal and northwestern faults control the Pleistocene river valleys and exhibit traces of the Holocene movements. On the Hangai-Hentei tectonic saddle deformations are often not conformal to the topography that existed in the Pliocene and even in the Pleistocene. That is, the most of the discontinuous deformations here are younger than the topography elements of the large valleys they intersect. With a certain degree of caution we can conclude that the beginning of the last stage of the activation of the movements along the faults or at least its main phase refers to the Late Pleistocene.

The kinematics of the Hangai-Hentei saddle faults and their morphogenetic types are associated with their strike. The latitudinal and WNW faults have the left-lateral strike-slip displacements with the revers or thrust vertical component. The horizontal component of the displacements as a rule exceeds the vertical one. The faults with the NW strike at the last stage of tectonic activation (Pleistocene-Holocene) are the revers fault and thrusts with the left-lateral and, in the deviation to the north, the right-lateral strike-slip component. Finally the faults with NE strike distributed mainly within the Hangai dome are represented by the normal faults (Fig. 2). The kinematics of the Burgut block faults are determined quite unambiguously. The revers movements along the NW striking faults and the right-lateral strike-slips along the faults with the submeridional strike are prevailing here (Fig. 2).

Within the Buren-Nuruu uplift the active faults with the sublatitudinal and northeastern strike have the maximum development (Fig. 2). The former are characterized by the left-lateral strike-slip

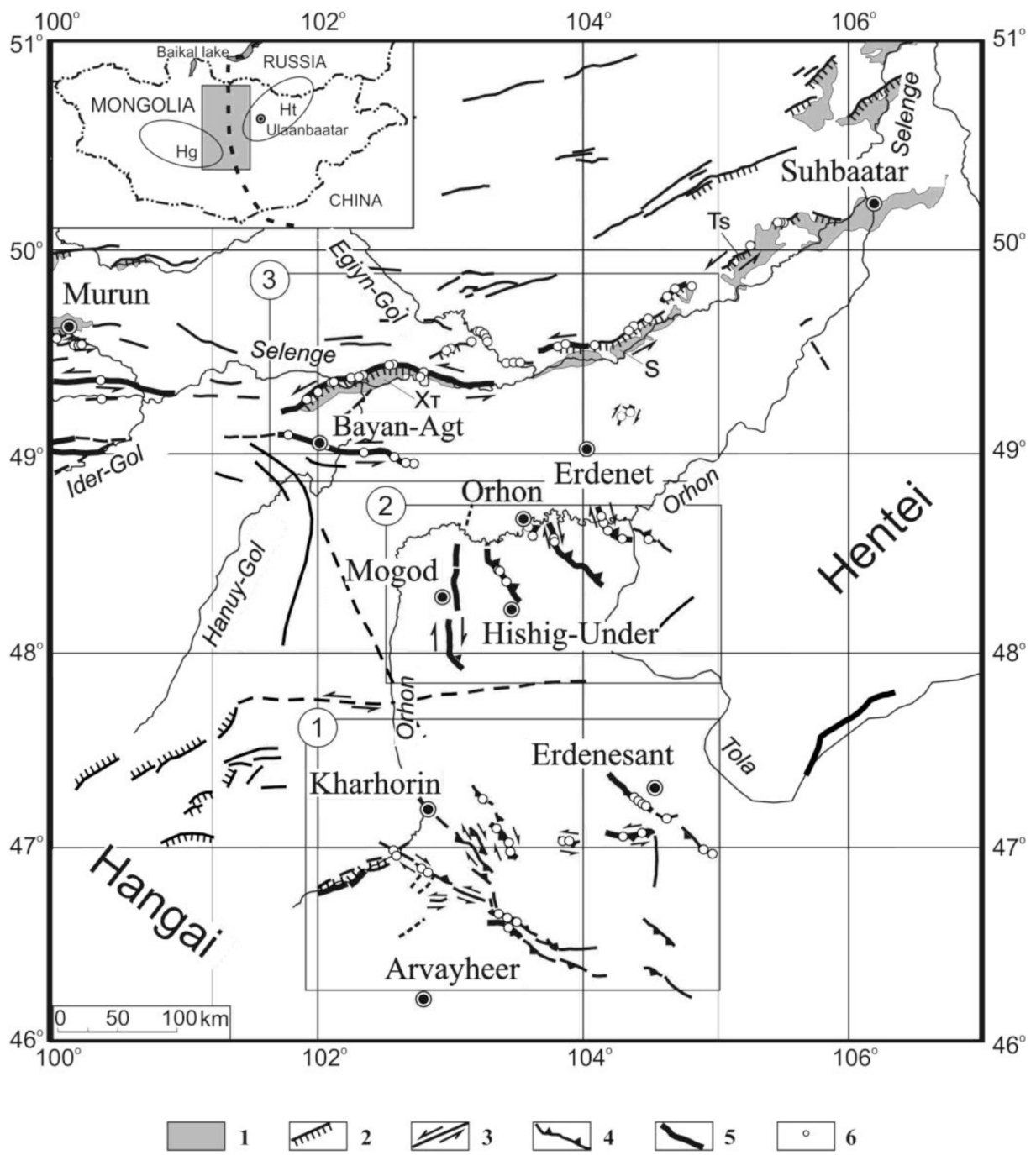


Figure 1: Scheme of faults of the Pliocene-Quaternary and Holocene activation of the central part of Mongolia. – Pliocene-Quaternary basins; 2–4 – fault kinematics: 2– normal fault, 3– strike-slip, 4– reverse fault and thrust; 5– faults with signs of the Holocene motions; 6– sites of observation. The shaded area in the diagram is the zone of possible position of the Amur plate boundary [Zonenshain, Savostin, 1981]. Inset: the study area (rectangle) and the position of the western boundary of the Amur lithospheric plate. Ellipses indicate the positions of the Hangai (Hg) and Hentei (Ht) domes.

displacements with the normal or reverse components depending on their deviation to the north-east or north-west strike respectively. Within the Selenga depression, a combination and mutual transitions of the sublatitudinal and northeastern faults are observed. The northeast faults are represented by the normal faults and left-lateral strike-slip faults. From the west to the east of the area their number increases. Such combination of the active faults is typical for the releasing band structure formed on the latitudinal left-lateral strike-slip [Parfeevets, Sankov, 2012].

The reconstructions of the stress state with the determination of its type was carried out using

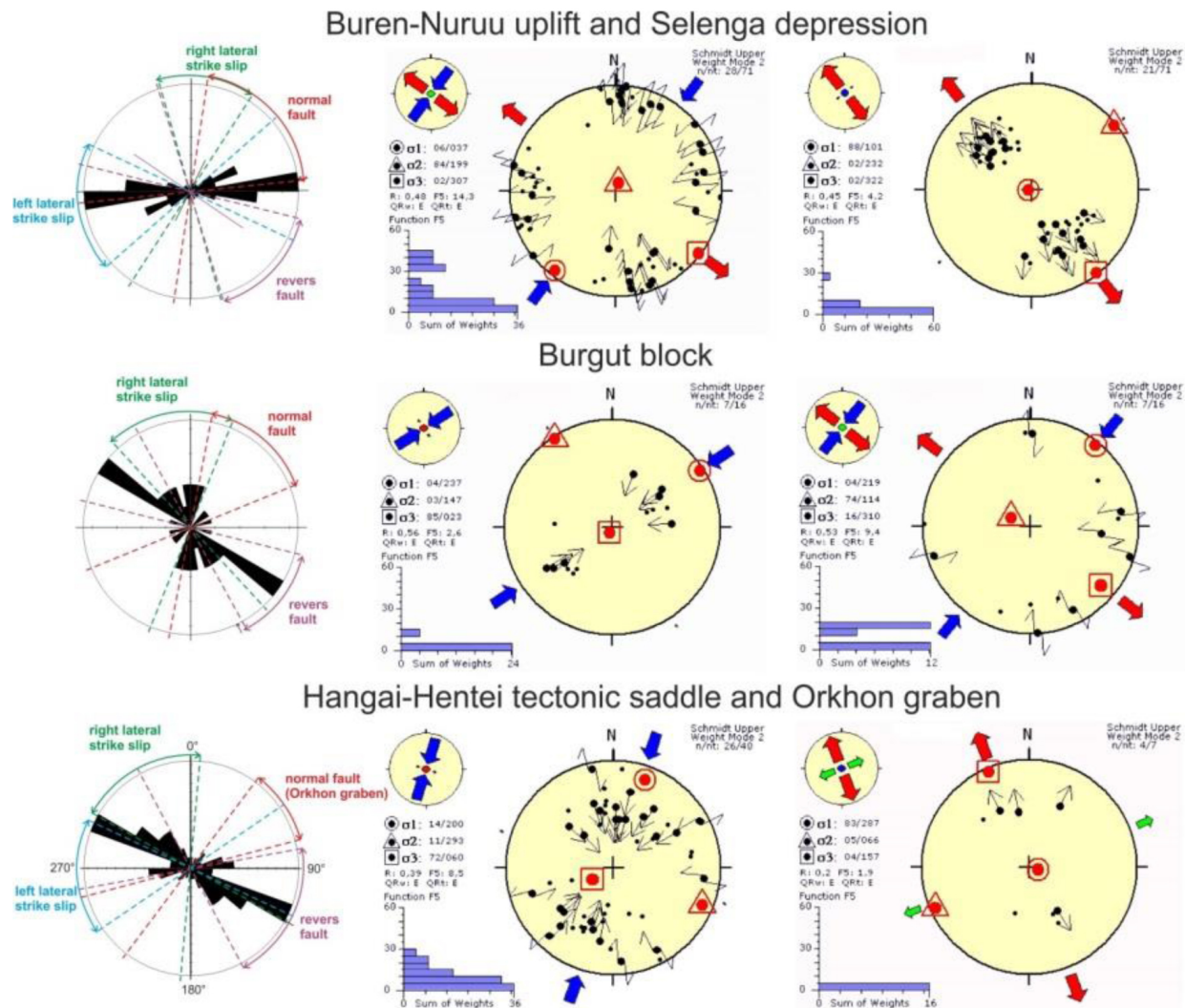


Figure 2: Faults kinematics and the results of the Late Cenozoic crustal stress reconstruction of the Central Mongolia. Left column – rose-diagrams of the active fault directions; central column – reconstructions of the prevailing stress tensor; right column – reconstructions of the secondary stress tensor.

data on the tectonic fracturing and fault displacements. Using all available solutions of the local stress tensors for the last stage of the deformations from the observations established at each site (Pleistocene-Holocene), we estimated the average stress tensor of the tectonic stress field (Fig. 2). For the Hangai-Hentei tectonic saddle the axis of maximum compression is subhorizontal and oriented to NNE. The minimal compression axis is subvertical (the compressive type of the stress tensor). For the Orkhon graben the extension axis (the minimum compression) is subhorizontal and oriented to NNW and the maximum compression axis is subvertical (the extensive type of the stress tensor).

The paleostress state of the earth's crust of the Burgut block is well described by the tensors of the compression and strike-slip types (Fig. 2), which are characterized by a subhorizontal position of the maximum compression axis oriented to the NE. The coincidence of the position of the axes of the main normal compressive stresses and the "re-indexing" of the axes σ_2 and σ_3 clearly shows that here the leading axis is the horizontal compression. This compression on the faults with the NW and submeridional strikes is realized in the thrust and strike-slip displacements respectively. The data of the palaeostresses reconstructions in the Mogod basin according to [Complex ..., 2004] coincide with the data noted above for the average direction of the maximum compression axis but more vary in the types of the stress tensors.

The similar situation is observed within the Buren-Nuruu block and Selenga depression (Fig 2). The strike-slip conditions with NNE direction of the maximum compression axis are dominated here.

The extension type of the stress field with NW direction of the minimum compression axis is the secondary. Both tensors have the same direction of the minimum compression axes. The vertically directed σ_1 and σ_2 axes have close values and replace each other.

Conclusions

The boundary between the Amur plate and the Mongolian block (according to [Sonenshain, Savostin, 1981]) is fragmentarily expressed in the tectonic structure and represents the marginal part of the active deformation zone. The faults of the territory inherit the ancient linear inhomogeneities of the Paleozoic and Mesozoic ages. The normal faults of the Orkhon graben that are laid independently of the ancient structures are the exceptions.

The beginning of the neotectonic activation of the faults varies from the Miocene in the Orkhon graben and the Pliocene in the Selenga depression to the late Pleistocene in the Hangai-Hentei tectonic saddle. The traces of the Holocene fracture activity were found at many sites.

The active faults of the Hangai-Hentei tectonic saddle and the Burgut block form clusters. Among them the strike-slips and strike-slips with the revers component of the displacements dominate. The kinematics of the strike-slip displacement depends on the strike of the fault. The faults of the Selenga depression are concentrated in the extended zones such as the releasing band. Here the left-lateral strike-slips and normal faults prevail.

The reconstruction of the paleostress shows that the area between the Amur plate and the Hangai block is deformed under the compression and strike-slip conditions. We can note a change from south to north of the strike of the maximum horizontal compression axis from NNE to NE. The conditions of extension and strike-slip are established in the Selenga depression and within the East Hangai uplift.

The reported study was funded by RFBR according to the research project 17-05-00826.

References

- [1] Complex geophysical and seismological investigations in Mongolia, 2004. Editors-in-chief V.I. Dzhurik and T. Dudarmaa. Ulaanbaatar-Irkutsk. 315 p.
- [2] Cunningham W.D., 2001. Cenozoic normal faulting and regional doming in the southern Hangay region, Central Mongolia: implications for the origin of the Baikal rift province // Tectonophysics. Vol. 331. P. 389-411.
- [3] Delvaux D. Release of Program Win-Tensor 4.0 for Tectonic Stress Inversion: Statistical Expression of Stress Parameters, 2012. Geophysical Research Abstracts. V. 14. EGU General Assembly, Vienna (EGU2012-5899).
- [4] Geological map of Mongolia. Scale 1:1000000. Ulaanbaatar, 1998.
- [5] Khilko S.D., Kurushin R.A., Kochetkov V.M. et al., 1985. Earthquakes and the basics of seismic zoning of Mongolia. Moscow, Nauka Publishing House, 224 p. (in Russian)
- [6] One century of seismicity of Mongolia / Dugarmaa T. and Shlupp A. – eds., Ulaanbaatar, CAG MAS. 2000.
- [7] Parfeevets A.V., Sankov V.A., 2012. Late Cenozoic tectonic stress fields of the Mongolian microplate. Comptes rendus – Geoscience. V. 344. P. 227-238.
- [8] Rasskazov S.V., Chuvashova I.S., Yasnygina T.A. Fefelov N.N., Saranina E.V. Potassium and potassium-soda volcanic series in the Cenozoic of Asia, 2012. Novosibirsk, GEO Akademic Publishing House. 310 p. (in Russian)
- [9] Zonenshain L. P., Savostin L. A., 1981. Geodynamics of the Baikal rift zone and plate tectonics of Asia. Tectonophysics. Vol. 76, N 1. P. 1–45.

CONTENTS

Astronomy, astrophysics and space science	09
Owl telescope in Mongolia	11
Observation of the coronal green line at a wavelength of 5303Å	12
The results of wavelet analysis application to variations of the Earth rotation parameters	13
Observation of solar radio bursts	14
The minor planets in the solar system	15
Intensity of solar ultraviolet radiation in Ulaanbaatar regions and comparative analysis of some characteristics of climatic conditions in the places of Khurel-Togoot and Tavan tolgoi	16
A fuzzy neural network model in analyzing the air pollution factors	19
Dynamic phenomena in the active regions of 24-th solar cycle	26
The optical afterglow observations of gamma-ray bursts	31
Solar active phenomena observation	32
Meteor observation in Irkutsk region	33
Mongolian-Russian cooperation at the Khurel-Togoot observatory in the ison project framework ..	34
A study of image prediction for yield mapping in real environment	35
 Geomagnetism	 41
Monitoring of the geomagnetic field variations at the high - mountain biospheric station dzhuga and forecasting of natural disasters and extreme weather	43
Probing the Earth's mantle using satellite and ground - based magnetic data. Progress status and challenges	44
Towards geophysical exploration of geothermal resources in the Hangai Mountains	45
High-precision Overhauser magnetometers applications	46
Variations of earthquake focal mechanism types in northern tien shan	53
Tectonomagnetic monitoring of crustal stress state in the baikal rift zone and some results for study of the kultuk earthquake	54
Rigid blocks in the earth's crust and strong earthquakes	59
The monitoring of geomagnetic field in the Baikal-Hubsugul fault in 2010-2015	63
Geophysical complex ISTP SB RAS for monitoring electromagnetic fields in high and middle latitudes ..	64
Study of the Magnetic Field Response due to Geodynamic Processes in Central Mongolia (Emeelt) and Russia (North-West Caucasus)	65
The heat flows via CPD	74
 Geodynamics, active deformation, GPS, active fault, paleoseismology	 79
Identification and characterization of the Sharkhai and Avdar active faults near Mongolia's capital city: Impact on Seismic Hazard Assessment in a low deformation setting	81
Co-seismic moment released by the surface rupturing 1934 bihar-nepal earthquake	87
Stress fields in the area of the Mogod earthquake in Mongolia from the structural paragenetic analysis of tectonic fracturing	88
Wave dynamics of rock deformations according results of monitoring	94
Numerical reconstruction of normal-fault scarps evolution	99
Radon monitoring of ulaanbaatar region	103
Cosmogenic ^{36}Cl geochronology of offset terraces along the Ovacık Fault (Malatya-Ovacık Fault Zone, Eastern Turkey): Implications for the intraplate deformation of the Anatolian Scholle	104
Tropospheric delay of GPS signals and their connection with the level of moisture content within the Baikal region and the Selenga river basin	105
Geodynamics of northern Mongolian and Transbaikalian segments of the Central Asian Orogenic Belt at	

<i>Late Paleozoic – Mesozoic</i>	111
<i>GPS developments in mongolia and its applications in geodynamic studies</i>	112
<i>Gheological hazard assessment of the Ulaanbaatar agglomeration</i>	113
<i>Structural characteristics of the Hovd fault zone, Mongolian Altaid region, western Mongolia</i>	114
<i>Cumulative deformation by multiple surface-faulting earthquakes on the Bulnay Fault, Mongolia: A preliminary investigation</i>	120
<i>Mapping of active faults in Korea by airborne LiDAR survey: A preliminary investigation</i>	121
<i>Slip rates and ages of past earthquakes along the main western Gobi-Altay active slip faults (Gobi-Altay, Mongolia)</i>	122
<i>Quantifying the differential uplift on the western branches of the north Anatolian fault: Sakarya river terraces, NW turkey</i>	124
<i>Horizotal slip distribution through several seismic cycles the eastern Bogd fault, Gobi-Altai, Mongolia</i>	129
<i>Impact of cosmic factors on the Baikal rift zone seismic regime</i>	131
<i>Studying active faults by GPR technique; example of Songino fault Ulaanbaatar</i>	137
<i>Present-day movements of the earth's crust of Mongolia from GPS measurements at the permanent sites</i>	143
<i>First results of GPS measurements within the local networks in the Central Mongolia</i>	147
<i>Songino active fault from GPR imaging and trench results, Ulaanbaatar, Mongolia</i>	152
<i>The crustal state of stresses and the conditions of the tectonic structures activation of Southeast Mongolia in the Cenozoic</i>	158
<i>Recurrence of strong earthquakes in the active Hovd fault zone, Mongolian Altay</i>	163
<i>Tectonic position and geological manifestations of the 1967 Mogod earthquake, Mongolia</i>	165
<i>Estimation of the recent activity of large faults in the Ulaanbaatar and Mogod geodynamic testing areas in Central Mongolia based on soil-radon data</i>	166
<i>Active faults and Late Cenozoic crustal stress state in the central part of Mongolia</i>	171
<i>Wave dynamics of seismicity in the annual cycles in the southeastern segment of the Amurian plate</i>	176
<i>High-resolution surface rupture map and slip distribution of the 1905 $M \geq 8$ Tsetserleg-Bulnay strike-slip earthquake sequence, Mongolia</i>	181
<i>Intraplate geodynamics in Mongolia: constraints from geochronology, thermochronology, and geochemistry</i>	182
Large intra-continental earthquakes: Source characteristics, seismic activity, historical earthquakes	183
<i>Preliminary result of earthquake hypocenter determination using new 1d velocity model: khuvsugul area</i>	185
<i>Seismicprofiling in a zone of mogod fault</i>	186
<i>Mongolian National Seismic Network and its operations</i>	189
<i>Lg-wave cross correlation applied to detection and location of events in high-seismicity regions of mainland east asia</i>	190
<i>Earthquake Monitoring: Automatic processing at the Mongolian National Seismic Network</i>	196
<i>Tectonophysical analysis of seismic hazard of faults in Central asia</i>	197
<i>Focal mechanisms of aftershocks of $Mw = 4.59$, Bayanbulag earthquake</i>	198
<i>A mechanism causing temporal variation in b-values Prior to a mainshock</i>	199
<i>Ambient noise monitoring in Ulaanbaatar region</i>	203
<i>Paleoseismic investigation on the eastern end of the Altyn Tagh fault</i>	207
<i>Seismic activity of the Emeelt fault area investigated using tomoDD</i>	208
<i>The seismicity of the south Hangay dome of central Mongolia: 1-d velocity model for the area from local earthquake data</i>	209

<i>Radionuclide analysis of the CTBTO's IMS stations data in Mongolia</i>	210
<i>Reference one dimensional velocity model and precise locations of local earthquake hypocenters in the hangay region</i>	211
<i>Precise location of seismicity in and around Bulnay fault</i>	212
<i>Detection capability of infrasound station</i>	213
<i>Ground Penetrating Radar result of data analysis For Songino active fault, Ulaanbaatar</i>	214
<i>Discrimination of earthquakes and explosions around north korean nuclear test site</i>	215
<i>Crustal and lithosphere structures</i>	221
<i>Deep structure of the baikal rift system Based on the seismic wave attenuation</i>	223
<i>Deep velocity structure and anisotropic properties of the asian upper mantle</i>	228
<i>Investigation of the boundary and internal fault zones of Tunka basin (Baikal rift system) using HVSR method</i>	231
<i>High Topography and Deformation in Continental Interiors: Structure and Geodynamics of Central Mongolia</i>	235
<i>Thickness of earth's crust under broadband stations of Mongolian seismic network</i>	236
<i>Estimation of coda wave attenuation in the Hangay Dome, central Mongolia</i>	240
<i>Crust and Upper Mantle Structure of Central Mongolia</i>	241
<i>Receiver function imaging of crustal and upper mantle structure beneath seismic station Ulan-Ude (Transbaikalia, Russia)</i>	247
<i>On conditions of preparation for the catastrophic earthquakes foci within earth crust of central asia</i>	250
<i>Deep configuration of the southeast edge of the siberian craton along the passcal_1992 transect</i>	256
<i>Vibroseismic sounding of the earth's crust on the profile Baikal – Ulaanbaatar</i>	261
<i>Study seismic activity in Khovd region (West part of Mongolia) and seismic velocity 1D model.</i>	266
<i>Seismic hazard assessment, strong ground motion, attenuation and site effects, microzoning</i>	271
<i>Seismic hazard assessment of bayan-ulgii aimag: Probabilistic analysis</i>	273
<i>Seismic hazard assessment of bayan-ulgii aimag: Microzoning mapping</i>	277
<i>Reducing Digitiser Latency for Earthquake Early Warning: New Strategies for Seismic Hardware</i>	282
<i>Prediction of seismic effects of large earthquakes in Mongolian-Siberian region by studying the dynamic parameters of earthquakes.</i>	283
<i>Paleoseismogenic deformations of the central Mongolia and seismic hazard assessment for Ulaanbaatar</i>	287
<i>Site effect estimation of Bayan-Ulgii aimag</i>	288
<i>Studying of tectonic infringements in seismically active areas of Mongolia.</i>	290
<i>Effects and Post-Disaster Actions during the 2015 Mw = 8.4 Northern Chile Earthquake.</i>	295
<i>Weather-climatic changes in the Baikal-Mongol region: analysis and forecast before 2050</i>	296
<i>The seismic microzoning study in Mongolia: the example of Ulgii city, center of Bayan-Ulgii aimag.</i>	302
<i>Seismic hazard assessment of bayan-ulgii aimag: Deterministic analysis</i>	306
<i>Seismic safety assessment of earth dams.</i>	309
<i>Seismic microzoning on the joint of geotechnical lands-capes.</i>	310
<i>Seismic Microzonation: principles and practices (for example, the city of Ulan-Ude).</i>	325
<i>Cosmogenic ^{36}Cl geochronology of offset terraces along the Ovacık Fault (Malatya-Ovacık Fault Zone, Eastern Turkey): Implications for the intraplate deformation of the Anatolian scholle</i>	330